Halogen radicals contribute to photooxidation in coastal and estuarine waters

Kimberly M. Parker[a] and William A. Mitch[a,1]

[a]Department of Civil and Environmental Engineering, Stanford University, Stanford, CA 94305

Edited by Donald E. Canfield, Institute of Biology and Nordic Center for Earth Evolution, University of Southern Denmark, Odense M., Denmark, and approved April 11, 2016 (received for review February 15, 2016)

Although halogen radicals are recognized to form as products of hydroxyl radical (•OH) scavenging by halides, their contribution to the phototransformation of marine organic compounds has received little attention. We demonstrate that, relative to freshwater conditions, seawater halides can increase photodegradation rates of domoic acid, a marine algal toxin, and dimethyl sulfide, a volatile precursor to cloud condensation nuclei, up to fivefold. Using synthetic seawater solutions, we show that the increased photodegradation is specific to dissolved organic matter (DOM) and halides, rather than other seawater salt constituents (e.g., carbonates) or photoactive species (e.g., iron and nitrate). Experiments in synthetic and natural coastal and estuarine water samples demonstrate that the halide-specific increase in photodegradation could be attributed to photochemically generated halogen radicals rather than other photoproduced reactive intermediates [e.g., excited-state triplet DOM (^{3}DOM*), reactive oxygen species]. Computational kinetic modeling indicates that seawater halogen radical concentrations are two to three orders of magnitude greater than freshwater •OH concentrations and sufficient to account for the observed halide-specific increase in photodegradation. Dark •OH generation by gamma radiolysis demonstrates that halogen radical production via •OH scavenging by halides is insufficient to explain the observed effect. Using sensitizer models for DOM chromophores, we show that halogen radicals are formed predominantly by direct oxidation of Cl^- and Br^- by ^{3}DOM*, an •OH-independent pathway. Our results indicate that halogen radicals significantly contribute to the phototransformation of algal products in coastal or estuarine surface waters.

halogen radicals | photochemistry | domoic acid | dimethyl sulfide | dissolved organic matter

Research on the photochemical transformation of organic compounds in seawater has focused on freshwater-relevant pathways, including direct photolysis and dissolved organic matter (DOM)-sensitized indirect photodegradation by excited triplet state DOM (^{3}DOM*) or reactive oxygen species [e.g., hydroxyl radical (•OH)] (1). High halide concentrations, the key characteristic distinguishing seawater from freshwater, are the predominant sink for •OH in seawater, with Br^- scavenging ~93% (Eq. **1**) (2), resulting in an ~40-fold reduction in •OH concentrations.

$$^{\bullet}OH + Br^- \rightarrow Br^{\bullet} + OH^-. \quad [1]$$

The role of the resultant $Br^{\bullet}$, as well as other radical reactive halogen species (RHS) (e.g., $Cl^{\bullet}$, $Cl_2^{\bullet-}$, $Br_2^{\bullet-}$, $ClBr^{\bullet-}$), in seawater photochemistry has received little attention. Here we evaluate the contribution of RHS, a family of photooxidants specific to seawater, to the photodegradation of important marine products for two reasons. Unlike diffusion-limited •OH rate constants, RHS rate constants with organic molecules span orders of magnitude (3), such that conversion of •OH to RHS focuses oxidation on more reactive molecules relative to bulk DOM. Secondly, direct halide oxidation by ^{3}DOM*, previously demonstrated using model triplet sensitizers (4, 5), may provide a seawater-specific, •OH-independent RHS production pathway that could increase overall radical generation rates.

We investigated the importance of RHS for photooxidation of dienes and thioethers. Dienes occur in biomolecules (e.g., fatty acids) and in the marine algal toxin (6, 7), domoic acid (Fig. 1*A*, *ii*), where the diene contributes to toxicity (8). During summer 2015, a large bloom of the marine diatom *Pseudo-nitzschia*, extending from central California to Alaska, led to significant concern regarding the production of domoic acid, a potent neurotoxin (9). Consumption of mollusks and fish contaminated with domoic acid has caused deaths and neurological damage in humans (6, 7), seabirds (10), and marine mammals (11). Dissolved domoic acid can affect marine microbial ecology by ligating micronutrients [e.g., iron (12)] and suppressing grazing by krill (13) and copepods (14). Although biological degradation in the water column has not been reported, both direct (15) and indirect (16) photodegradation contribute to domoic acid loss in seawater. These studies have not considered the role of RHS oxidation in domoic acid photodegradation.

Thioethers occur in the amino acid methionine and the marine algal product dimethyl sulfide (DMS) (Fig. 1*A*, *iv*). DMS is the primary natural marine sulfur source to the atmosphere, playing a critical role in cloud condensation nuclei formation and thereby affecting atmospheric albedo (17–19). Previous research indicated that phototransformation accounts for 20–90% of DMS degradation in seawater, with the remainder due to biological degradation (20). Laboratory studies suggested that RHS formed by nitrate photolysis in the presence of seawater Br^- (via •OH) could promote DMS photodegradation, indicating a possible role for RHS-mediated DMS oxidation (21). However, field measurements suggest that, except for high-nitrate, low-DOM waters (22), DOM is the primary photosensitizer contributing to DMS photodegradation in natural waters (23, 24), indicating a need to clarify mechanisms responsible for DMS photodegradation in surface seawaters (1). For each compound class, we evaluated

Significance

Scavenging by halides to produce halogen radicals is recognized as a significant sink for hydroxyl radical (•OH) in seawater. However, the contribution of halogen radicals to the transformation of marine organic constituents has not been explored. Here, we demonstrate that halogen radicals are formed predominantly by direct oxidation of seawater halides (i.e., Cl^-, Br^-) by excited-state triplet dissolved organic matter chromophores, an •OH-independent pathway. The resulting halogen radicals increase photochemical transformation rates of important algal products, including dimethyl sulfide and the neurotoxin domoic acid, by up to fivefold relative to freshwater conditions. The contribution of halogen radicals to the photochemical transformation of critical marine organic compounds may have important implications for biogeochemical processes in coastal and estuarine waters.

Author contributions: K.M.P. and W.A.M. designed research; K.M.P. performed research; K.M.P. and W.A.M. analyzed data; and K.M.P. and W.A.M. wrote the paper.

The authors declare no conflict of interest.

This article is a PNAS Direct Submission.

[1]To whom correspondence should be addressed. Email: wamitch@stanford.edu.

This article contains supporting information online at www.pnas.org/lookup/suppl/doi:10.1073/pnas.1602595113/-/DCSupplemental.

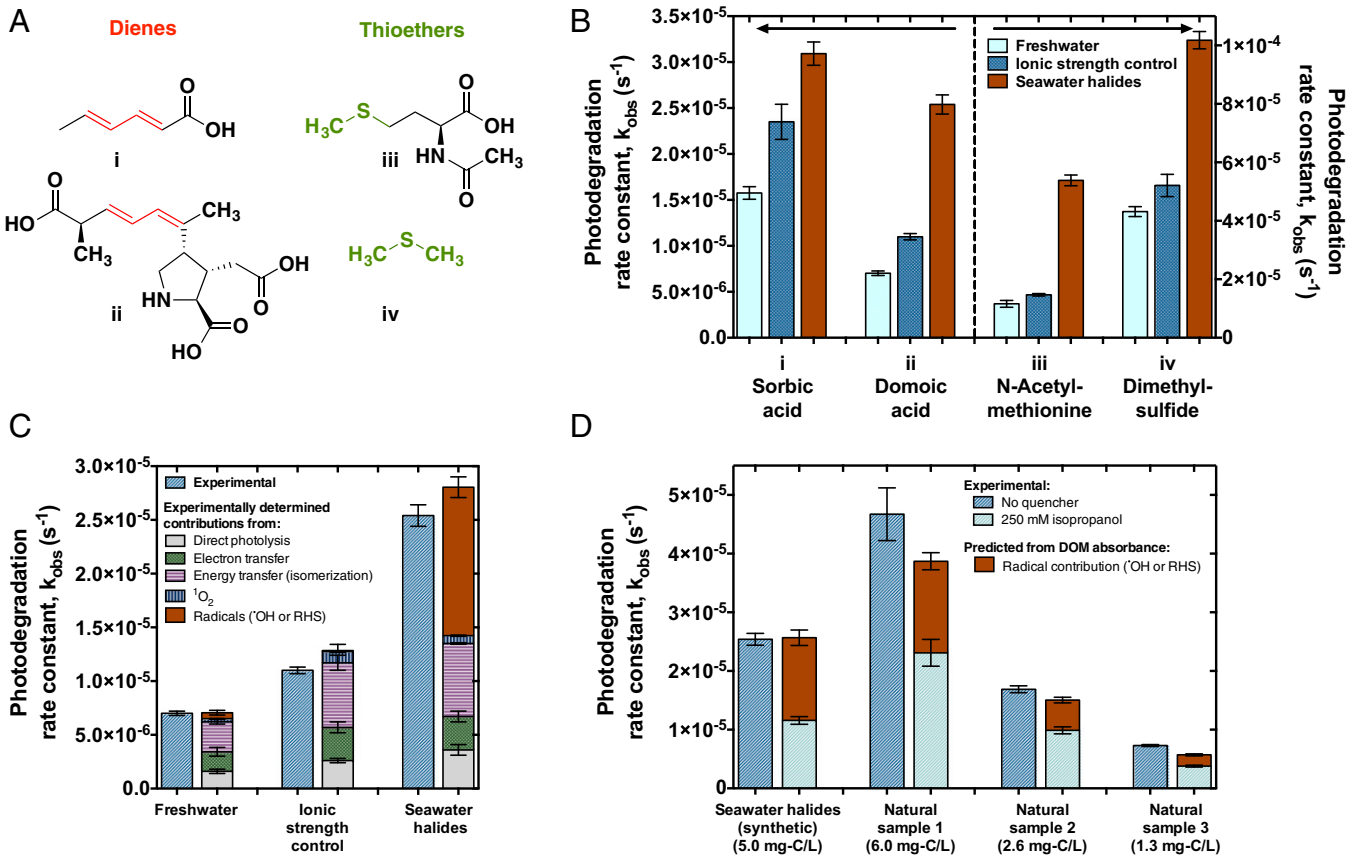

Fig. 1. Photodegradation of organic compounds in synthetic and natural water matrices. (*A*) Chemical structures of dienes and thioethers. (*B*) Pseudofirst-order photodegradation rate constants of dienes and thioethers in synthetic matrices sensitized by 5 mg/L Suwannee River DOM at pH 8.1 with 20 mM phosphate buffer alone (freshwater), with 540 mM $NaClO_4$ (ionic strength control), or with 540 mM NaCl and 0.8 mM NaBr (seawater halides). (*C*) Experimental domoic acid photodegradation rate constants and attributions to specific degradation pathways. (*D*) Experimental domoic acid photodegradation rate constants in synthetic and natural water samples with and without 250 mM isopropanol as a radical quenching agent. Radical contributions in each sample were predicted from the rate of photon absorbance by DOM in each sample and the quantum yield of radical-mediated domoic acid photodegradation determined using the radical contribution quantified in synthetic seawater solutions. Error bars represent the SE of the slope obtained by linear regression of duplicate sets of semilog transformed kinetic data.

structural analogs with known RHS rate constants [i.e., sorbic acid (25), Fig. 1*A*, *i*: $k(Cl_2^{\bullet-}) = 6.8 \times 10^8\ M^{-1}{\cdot}s^{-1}$; *N*-acetylmethionine (26), Fig. 1*A*, *iii*: $k(Br_2^{\bullet-}) = 3.0 \times 10^9\ M^{-1}{\cdot}s^{-1}$].

Results and Discussion

Effect of Halides on Photodegradation. First, we investigated diene and thioether photodegradation in synthetic freshwater and seawater solutions to isolate the impact of halides. In solutions containing 5 mg/L Suwannee River DOM at pH 8.1 illuminated by a solar simulator, the pseudofirst-order photodegradation rate constants (k_{obs}) increased by factors of 2–5 from synthetic freshwater to seawater (540 mM Cl^- and 0.8 mM Br^-) (Fig. 1*B*). In ionic strength controls, k_{obs} for dienes increased by factors of 1.5–1.6 relative to the freshwater case, but ionic strength had less effect for thioethers.

Additional experiments delineated specific pathway contributions to domoic acid photodegradation, including direct photolysis (DOM-free experiments), singlet oxygen [$^1O_2$; deuterium oxide experiments (27)], and ^{3}DOM* electron transfer (i.e., oxidation) reactions [phenol and alcohol quenching experiments (28)] (Fig. 1*C* and *SI Appendix*, *Contribution of Photochemical Pathways*). The ^{3}DOM* also can transfer energy to domoic acid, a *cis–trans* diene, forming geometric isomers (29). As observed previously with sorbic acid (30), the domoic acid isomerization rate doubled between freshwater and the ionic strength control or seawater halides (*SI Appendix*, Fig. S1 *E* and *F*), accounting for the ionic strength-specific rate increase. Although the role of radicals (alcohol quenching experiments; *SI Appendix*, Table S1) was minor in halide-free solutions, their importance increased by 25-fold or more in the presence of halides, completely accounting for the seawater halide-specific effect (Fig. 1*C*). These results suggest that freshwater radicals (e.g., $^{\bullet}$OH) were relatively unimportant, whereas RHS could contribute significantly to domoic acid photodegradation in seawater. Additional experiments validating these conclusions are discussed in *Elucidation of Radical Intermediates*.

Highlighting the importance of Cl^- and Br^- among seawater ions, the domoic acid photodegradation rate was the same in the presence of seawater-relevant halide concentrations or full synthetic seawater, containing seawater-relevant halide concentrations as well as other major salts present in seawater (*SI Appendix*, Fig. S2). The importance of DOM for radical production was suggested by the lack of significant increase in domoic acid photodegradation rates upon addition of nitrate (5–200 μM) and Fe^{3+} (2–10 nM) as initiators of $^{\bullet}$OH production (*SI Appendix*, Fig. S2).

Although synthetic solutions were used to isolate the role of halides, a similar importance for radical-mediated domoic acid degradation was found in natural coastal waters. Addition of 250 mM isopropanol as a radical quenching agent reduced domoic acid photodegradation rates by 40–50% in three California coastal waters (Fig. 1*D*) containing 1.3–6.0 mg C/L DOM, 3–175 μM

nitrate, and <20 nM iron (*SI Appendix*, Table S2). The contribution of radicals to k_{obs} in these coastal waters was well predicted by scaling the radical-associated k_{obs} for synthetic seawater (Fig. 1*C*) by the rate of photon absorbance by the solution (≤400 nm; *SI Appendix*, Fig. S3) in the natural waters (Fig. 1*D*), suggesting that DOM contributes to radical production.

Elucidation of Radical Intermediates. We sought to distinguish the contribution of $^{\bullet}OH$ and RHS to the radical-mediated photodegradation of domoic acid. Solar simulator illumination of bromoacetophenone (BrAP) produces $Br^{\bullet}$ [0.4 quantum yield (31)], which rapidly reacts with seawater halides (540 mM Cl^-, 0.8 mM Br^-) to form other RHS and with H_2O/OH^- to form $^{\bullet}OH$. While *tert*-butanol and methanol have been used to quench $^{\bullet}OH$, they also quench RHS, although less effectively. Application of 25 mM and 250 mM of either *tert*-butanol or methanol as radical quenchers resulted in ∼10–50% reduction in domoic acid photodegradation (Fig. 2*A*). A computational model (*SI Appendix*, *Reactions Included in Kinetic Model*) indicated that these quenchers would decrease domoic acid photodegradation by >85% if only $^{\bullet}OH$ oxidized domoic acid, but would approach the experimentally observed quenching (10–45%) if RHS reactions were considered (Fig. 2*A*). These results indicate that RHS can degrade domoic acid in an RHS-dominated system.

Considering the effect of a series of quenchers on domoic acid indirect photodegradation pseudofirst-order rate constants ($k_{indirect}$) in the presence of seawater halides, we found a strong linear correlation (R^2 = 0.87; P = 0.002) between rate constants observed in the BrAP-sensitized and the more complex DOM-sensitized matrices (Fig. 2*B*). Because these quenchers would almost completely scavenge $^{\bullet}OH$, the strong correlation and moderate reduction in $k_{indirect}$ indicate that RHS dominated the halide-specific component of domoic acid photodegradation sensitized by DOM.

Product Analysis. Liquid chromatography-mass spectrometry (LC-MS) analysis in the full-scan mode indicated that BrAP- and DOM-sensitized domoic acid ($[M+H]^+$ = 312) photodegradation in the seawater halides matrix did not generate products with the characteristic isotopic ratios of chlorinated or brominated compounds. For the DOM-sensitized matrices, a product ($[M+H]^+$ = 268) was observed in both the freshwater and seawater matrices (*SI Appendix*, Fig. S4). Previous research indicated that this product is a decarboxylation product of domoic acid (32). The lack of its detection in the BrAP-sensitized system suggests that this is not a product of RHS reactions but is a product of other photodegradation pathways. However, LC-MS analysis confirmed that BrAP- and DOM-sensitized domoic acid photodegradation in the seawater halides matrix generated the same predominant, but unidentified, product ($[M+H]^+$ = 344), which was not observed in DOM-sensitized freshwater or the ionic strength control (*SI Appendix*, Fig. S4). These results indicate that halides increase domoic acid photodegradation and alter its transformation pathway. The lack of detection of chlorinated and brominated products is consistent with previous research showing that, although halogenated byproduct formation is possible, RHS react predominantly by oxidation rather than halogen addition for some organic substrates (25, 33). For example, although engineered treatment of phenol by $^{\bullet}OH$ in the presence of seawater halides (which generates RHS) formed halophenols, the maximum yield was ∼0.5% (33).

Photochemical Generation of RHS. RHS formation via halide scavenging of $^{\bullet}OH$ (Eq. **1**) simply converts one radical oxidant to another. However, domoic acid photodegradation rates may increase in seawater relative to freshwater through conversion of $^{\bullet}OH$ to RHS because RHS more selectively target some organic constituents over DOM (3, 25). When $^{\bullet}OH$ was produced by gamma radiolysis in the presence of 5 mg/L DOM, domoic acid degradation doubled between an ionic strength control and a seawater halides matrix (*SI Appendix*, Fig. S5). However, methanol (25 mM) applied to sunlit DOM-sensitized solutions indicated a minor $^{\bullet}OH$

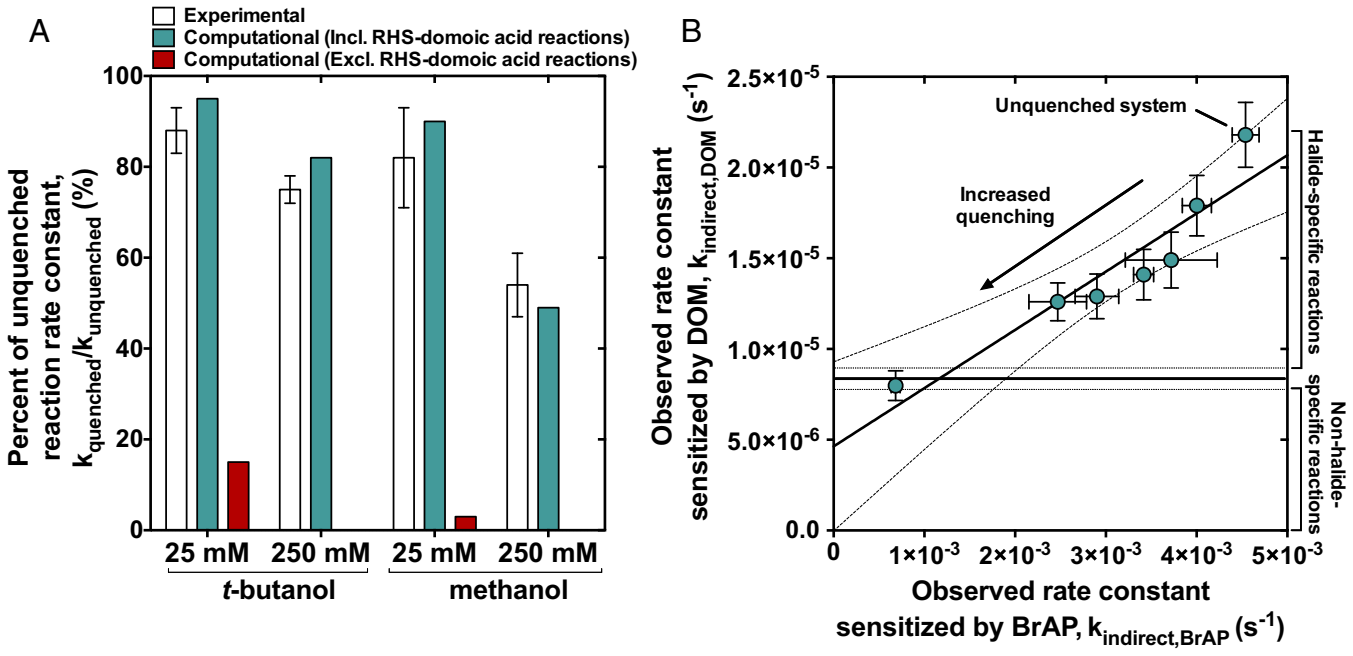

Fig. 2. Domoic acid photodegradation in the seawater halides matrix (540 mM Cl^-, 0.8 mM Br^-) in the presence of quenching agents. (*A*) Rate constants relative to unquenched rate constants sensitized by 100 μM bromoacetophenone (BrAP) obtained experimentally or by a computational model including domoic acid degradation via reactions with both $^{\bullet}OH$ and RHS or $^{\bullet}OH$ alone. (*B*) Correlation between rate constants of domoic acid degradation sensitized by 5 mg/L Suwannee River DOM versus degradation sensitized by 100 μM BrAP in the presence of radical quenching agents. Error bars represent the SE of the slope obtained by linear regression of duplicate sets of semilog transformed kinetic data.

contribution to domoic acid photodegradation in freshwater (Fig. 1*C*). If the freshwater pseudofirst-order rate constant for radical reactions were doubled in seawater (as observed using gamma radiolysis), conversion of $^{\bullet}$OH to RHS could at most account for 5(±4)% of the halide-specific increase in domoic acid photodegradation observed in seawater. These results suggest that conversion of $^{\bullet}$OH to more selective RHS alone is insufficient to account for the enhanced radical-mediated degradation of domoic acid in seawater.

We evaluated RHS production from direct halide oxidation by ^{3}DOM* as an alternative formation pathway in seawater. Transient spectroscopy demonstrated RHS formation from direct halide oxidation by synthetic aromatic ketone triplet sensitizers (^{3}SEN*) (4, 5), which may represent a component of natural DOM triplet sensitizers. Aromatic ketone triplet sensitizers form a charge transfer complex (exciplex) with halides, resulting in ^{3}SEN* quenching to the ground state (SEN) or charge separation to produce RHS (Eqs. **2** and **3**) (4). As the halide reduction potential decreases relative to the triplet sensitizer reduction potential, the exciplex activation free energy ($\Delta G^{\ddagger}$) decreases (Fig. 3*A*), favoring exciplex formation (*SI Appendix, Oxidation of Halides by Triplets*). Because $E^{\circ}_{Br/Br-}$ (1.92 V_{NHE}) < $E^{\circ}_{Cl/Cl-}$ (2.50 V_{NHE}), Br^- exciplexes are favored (4). However, halide concentrations also control radical yields. At <10 mM halides, exciplex quenching is favored (Eq. **2**). The greater spin–orbit coupling constant of Br^- compared with Cl^- promotes the intersystem crossing associated with quenching (34). At >100 mM halides, ternary exciplexes form, promoting RHS formation (Eqs. **3** and **4**) because the lack of spin–orbit coupling for the nascent dihalide radicals inhibits quenching via intersystem crossing. RHS formation by Eq. **3** is expected to dominate in seawater containing both Br^- and Cl^- due to the lower reduction potential of Br^-. However, RHS formation by Eq. **4** may also contribute because Cl^- concentrations in seawater are 675-fold higher than Br^-.

$$^3(\mathrm{SEN})^* + \mathrm{Br}^- \rightarrow {}^3(\mathrm{SEN\text{-}Br})^{*-} \rightarrow \mathrm{SEN} + \mathrm{Br}^- \quad [2]$$

$$^3(\mathrm{SEN})^* + \mathrm{Br}^- \rightarrow {}^3(\mathrm{SEN\text{-}Br})^{*-} + \mathrm{Cl}^- \rightarrow {}^3(\mathrm{SEN\text{-}Br\text{-}Cl})^{*2-} \rightarrow \mathrm{SEN}^{\bullet-} + \mathrm{BrCl}^{\bullet-} \quad [3]$$

$$^3(\mathrm{SEN})^* + \mathrm{Cl}^- \rightarrow {}^3(\mathrm{SEN\text{-}Cl})^{*-} + \mathrm{Cl}^- \rightarrow {}^3(\mathrm{SEN\text{-}Cl\text{-}Cl})^{*2-} \rightarrow \mathrm{SEN}^{\bullet-} + \mathrm{Cl}_2^{\bullet-}. \quad [4]$$

For aromatic ketone triplet sensitizers, the percentage changes in quantum yields for domoic acid photodegradation in the presence of halides relative to ionic strength controls were plotted versus triplet reduction potentials (Fig. 3*B*). For all sensitizers, 0.8 mM Br^- alone did not increase domoic acid photodegradation, suggesting that triplet quenching was favored over RHS formation. For 540 mM Cl^-, domoic acid photodegradation increased with ^{3}SEN* reduction potential, suggesting sufficient Cl^- concentration to promote $Cl_2^{\bullet-}$ formation. Quantum yields in solutions containing both 540 mM Cl^- and 0.8 mM Br^- were even higher than for Cl^- alone. The results are consistent with $BrCl^{\bullet-}$ formation due to favorable exciplex formation via the lower $\Delta G^{\ddagger}$ of ^{3}SEN*–Br^- interactions, and promotion of ternary exciplex formation by the high Cl^- concentration (Eq. **3**). The same trend was observed for 5 mg/L DOM (Fig. 3*C*). The increase in quantum yield was intermediate between those observed for acetophenone and benzophenone, suggesting triplet

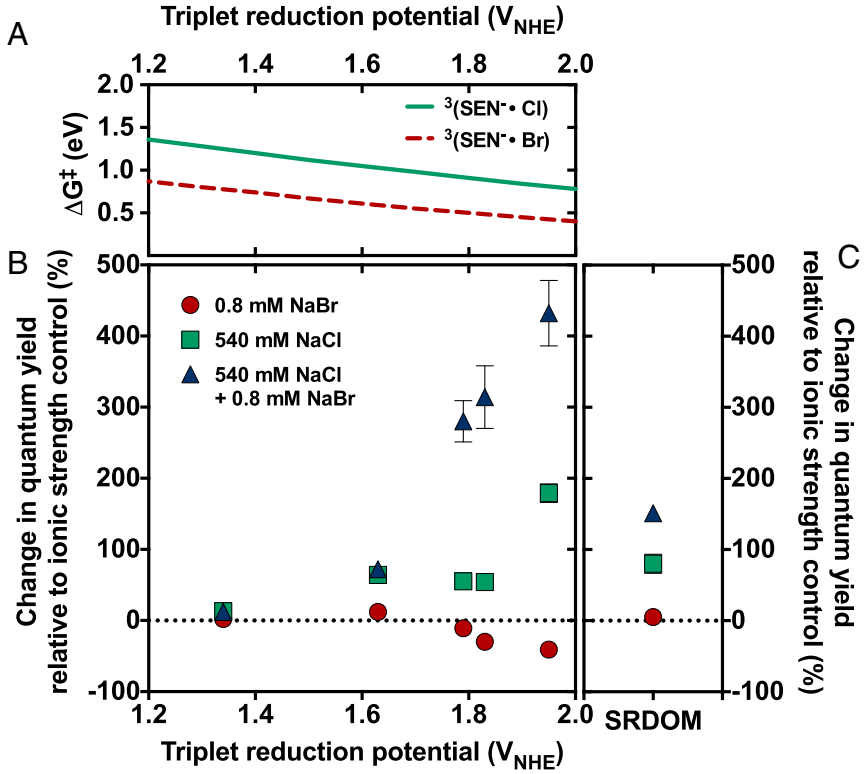

Fig. 3. Domoic acid photodegradation by ^{3}SEN* of varying reduction potentials (2-acetonaphthenone, 1.34 V_{NHE}; acetophenone, 1.63 V_{NHE}; benzophenone, 1.79 V_{NHE}; benzophenone-4-carboxylate, 1.83 V_{NHE}; and 3-benzoylpyridine, 1.95 V_{NHE}). (*A*) Calculated $\Delta G^{\ddagger}$ for charge transfer exciplex formation from ^{3}SEN* with Cl^- or Br^-. Percent change in domoic acid photodegradation quantum yields relative to the ionic strength control (540 mM $NaClO_4$) with varying halide conditions sensitized by (*B*) 50 μM synthetic triplet sensitizers or (*C*) 5 mg/L Suwannee River DOM. Error bars represent the SE of the slope obtained by linear regression of duplicate sets of semilog transformed kinetic data.

reduction potentials of ~1.6–1.8 V_{NHE}, concurring with previous estimates based on ^{3}DOM* reactivity with phenols (1.36–1.95 V_{NHE}) (35). However, it is important to note that aromatic ketones, whose halide oxidation capability has been validated (4, 5), may represent one of several components of ^{3}DOM*.

Radical Steady-State Concentrations. Although $^\bullet$OH steady-state concentrations are about one order of magnitude lower in seawater ($[^\bullet OH]_{SS} = 1.1 \times 10^{-17}$ M in seawater) than in freshwater (2), kinetic modeling estimates that RHS production offsets this loss, generating total RHS concentrations two to three orders of magnitude higher ($[RHS]_{SS} \approx 2 \times 10^{-14}$ M in seawater) (*SI Appendix*, Table S3). Although $ClBr^{\bullet-}$ is predicted to be the dominant RHS formed initially via halide oxidation by ^{3}DOM* (Eq. **3**), kinetic modeling indicates that $Br_2^{\bullet-}$ concentrations may exceed those of $ClBr^{\bullet-}$ by ~2.5-fold (*SI Appendix*, Table S3). Additional modeling indicated that the dominance of $Br_2^{\bullet-}$ arises from further reactions of $ClBr^{\bullet-}$ (e.g., with Br^-) (*SI Appendix*, Table S3). For model validation, we divided the experimental seawater-specific photodegradation pseudofirst-order rate constants for dienes and thioethers (Fig. 1) by modeled RHS concentrations (*SI Appendix*, Table S3) to estimate second-order rate constants for diene and thioether oxidation by the dominant RHS species ($Br_2^{\bullet-}$, $ClBr^{\bullet-}$) of 1–17 $\times 10^8$ $M^{-1}\cdot s^{-1}$ and 1–5 $\times 10^9$ $M^{-1}\cdot s^{-1}$, respectively. These values agree with previously reported values for sorbic acid and $Cl_2^{\bullet-}$ (6.8×10^8 $M^{-1}\cdot s^{-1}$) (25), and *N*-acetylmethionine and $Br_2^{\bullet-}$ (3.0×10^9 $M^{-1}\cdot s^{-1}$) (26). Note that indirect photodegradation of domoic acid by RHS exceeded that by direct oxidation by ^{3}DOM* (electron transfer) in synthetic seawater experiments (Fig. 1*C*). Previous research measured ^{3}DOM* steady-state concentrations of ~10^{-15} M under similar conditions (30). Thus, for compounds that are readily oxidized by RHS, oxidation by RHS may exceed transformation by direct reaction with ^{3}DOM*.

Implications. Our results indicate that halides present in seawater increase the photodegradation of dienes (e.g., domoic acid) and thioethers (e.g., DMS) by factors of 2–5, driven predominantly by RHS produced by direct halide oxidation by ^{3}DOM*. Beyond algal toxins and DMS, the prevalence of photoproduced RHS suggests their potential importance for turnover of marine organic constituents featuring RHS rate constants > 10^8 $M^{-1}\cdot s^{-1}$ in coastal or estuarine waters exhibiting sufficient DOM to promote indirect photolysis. Accordingly, photogenerated halogen radicals are expected to contribute to sulfur (21) and organic carbon (36) biogeochemical turnover in coastal waters, as well as the abiotic photohalogenation of marine organic matter (37, 38).

Our results also demonstrate the importance of direct halide oxidation by ^{3}DOM* for RHS generation in sunlit coastal waters. Although this research focused on seawater conditions, RHS formation from direct halide oxidation by ^{3}DOM* likely also applies to marine aerosols, where halide concentrations can exceed those in seawater (39, 40). Because nonradical dihalogen species form as products of radical RHS reactions [e.g., 2 $ClBr^{\bullet-} \rightarrow ClBr + Br^- + Cl^-$ (41)], this pathway may contribute to the release of halogens to the atmosphere, with implications for tropospheric ozone degradation (42) and the atmospheric mercury cycle (43).

Materials and Methods

Synthetic and Natural Matrices. Synthetic samples, including full synthetic seawater (420 mM NaCl, 0.8 mM NaBr, 29 mM Na_2SO_4, 54 mM $MgCl_2\bullet 6H_2O$, 11 mM $CaCl_2\bullet 2H_2O$, 10 mM KCl, 0.35 mM H_3BO_3, 1.8 mM $NaHCO_3$, and 0.26 mM Na_2CO_3) and samples amended with nitrate (5–200 μM) and iron (2–10 nM), were prepared using reagent-grade chemicals. Unless otherwise noted, Suwannee River natural organic matter (5 mg C/L) obtained from the International Humic Substances Society was used as a sensitizer in synthetic matrices. Natural waters were obtained as grab samples from locations in San Francisco Bay and Monterey Bay. Measured water quality parameters (i.e., salinity, organic carbon content, solution absorbance, pH, NO_3^-, Fe) are presented in *SI Appendix*, Table S2.

Photochemical Experiments. Photodegradation experiments were performed using a Q-SUN Xenon Test Chamber (Xe-1) solar simulator. The total photon flux for the system from wavelengths 280–700 nm was calculated to be 4.13×10^{-5} $mol_{photon}\cdot L^{-1}\cdot s^{-1}$ using *p*-nitroanisole/pyridine actinometry (44). Samples were stirred in 25-mL quartz test tubes held at a 30° angle from the reactor bottom. Temperature was held at 20 °C using a recirculating water bath. Aliquots were periodically sampled from the test tubes. Absorbance scans were taken during experiments using an Agilent Cary 60 UV-Vis spectrophotometer to ensure that sensitizer photobleaching was not significant during the course of the experiments.

Gamma-Radiolysis Experiments. Steady-state γ-radiolysis was performed using a Cesium-137 source with a dose rate of 270 R/min determined using Fricke dosimetry (45). Synthetic seawater samples (25 mL) containing 2 μM domoic acid were purged with nitrous oxide (N_2O) for 10 min before exposure to isolate $^\bullet$OH.

Analytical Methods. Sorbic acid degradation was monitored using an Agilent 1260 Infinity HPLC-UV equipped with an Inertsil ODS-3 C18 column using a previously reported method (46).

Using the same system, domoic acid concentrations were measured with an isocratic mobile phase (90% 25 mM formic acid in MilliQ water and 10% acetonitrile) at 1 mL/min (retention time = 23 min) and UV absorbance at 242 nm. Due to the low pK_a values for the three carboxylic acid functional groups in domoic acid (2.10, 3.72, and 4.97) (47), all domoic acid samples and standards were acidified with 50 mM phosphoric acid before analysis to improve peak shape. Domoic acid product analysis was performed using an Agilent 1260 HPLC coupled to a 6460 triple quadrupole mass spectrometry (MS) system. Product isomer identification was confirmed using positive mode (*m/z* 100–450) with the same column and isocratic mobile phase as HPLC-UV, but with reduced flow (0.5 mL/min). Detection of oxidation products was attempted in both positive (*m/z* 100–500) and negative (*m/z* 20–500) mode using a gradient method with 25 mM formic acid in MilliQ water and acetonitrile as the mobile phase.

N-acetylmethionine was analyzed using the HPLC-MS system equipped with an Agilent Poroshell 120 EC-C18 column and an isocratic mobile phase (98% 25 mM formate buffer in MilliQ water and 2% acetonitrile) at 0.4 mL/min (retention time = 4 min). Quantification was achieved in single ion monitoring mode (*m/z* = 190.2).

Samples containing DMS were spiked with 2 μM DMS-d_6 as an internal standard. Following the addition of sodium sulfate to saturation, liquid–liquid extraction was performed using methyl *tert*-butyl ether. Sample extracts were analyzed using gas chromatography mass spectroscopy (Agilent 240 GC-MS). Aliquots (5 μL) were injected in splitless mode (inlet temperature = 90 °C). The oven temperature was held at 30 °C for 5 min, then raised to 100 °C at 5 °C/min. Analytes were quantified under electron impact ionization in single ion monitoring mode (DMS, *m/z* = 47 + 62; DMS-d_6, *m/z* = 50 + 68).

Kinetic Model. Kinetic modeling was performed using the computer program Kintecus 4.55 (48). The model contains 166 inorganic reactions with rate constants obtained from the literature or estimated as detailed previously (32, 49). Previous work with phenol, for which reaction rate constants with many daughter radicals were available, indicated good agreement with experimental results (32). Reactions modeled between organic chemicals and radical species were added to the model with rate constants described in the *SI Appendix, Reactions Included in Kinetic Model*, and Table S4.

ACKNOWLEDGMENTS. The authors thank Dr. E. Kolodziej for comments. The authors acknowledge funding from the National Science Foundation (Grant CBET-1066526) and the Woods Institute for the Environment (Stanford University). K.M.P. was supported by a National Science Foundation Graduate Research Fellowship (Grant DGE-114747), the Abel Wolman Fellowship (American Water Works Association), and the Gerald J. Lieberman Fellowship (Stanford University).

1. Mopper K, Kieber DJ, Stubbins A (2015) *Marine Photochemistry of Organic Matter: Processes and Impacts. Biogeochemistry of Marine Dissolved Organic Matter*, eds Hansell DA, Carlson CA (Elsevier, New York), 2nd Ed, pp 389–450.
2. Mopper K, Zhou X (1990) Hydroxyl radical photoproduction in the sea and its potential impact on marine processes. *Science* 250(4981):661–664.
3. Neta P, Huie RE, Ross AB (1988) Rate constants for reactions of inorganic radicals in aqueous solution. *J Phys Chem Ref Data* 17(3):1027–1284.
4. Loeff I, Rabani J, Treinin A, Linschitz H (1993) Charge transfer and reactivity of $n\pi^*$ and $\pi\pi^*$ organic triplets, including anthraquinonesulfonates, in interactions with inorganic anions: A comparative study based on classical Marcus theory. *J Am Chem Soc* 115(20):8933–8942.

5. Jammoul A, Dumas S, D'Anna B, George C (2009) Photoinduced oxidation of sea salt halides by aromatic ketones: A source of halogenated radicals. *Atmos Chem Phys* 9(13):4229–4237.
6. Wright JLC, et al. (1989) Identification of domoic acid, a neuroexcitatory amino acid, in toxic mussels from eastern Prince Edward Island. *Can J Chem* 67(3):481–490.
7. Perl TM, et al. (1990) An outbreak of toxic encephalopathy caused by eating mussels contaminated with domoic acid. *N Engl J Med* 322(25):1775–1780.
8. Hampson DR, Huang X-P, Wells JW, Walter JA, Wright JL (1992) Interaction of domoic acid and several derivatives with kainic acid and AMPA binding sites in rat brain. *Eur J Pharmacol* 218(1):1–8.
9. Doughton S (June 15, 2015) Toxic algae bloom might be the largest one ever. *The Seattle Times*. Available at www.seattletimes.com/seattle-news/health/toxic-algae-bloom-might-be-largest-ever/.
10. Fritz L, Quilliam MA, Wright JLC, Beale AM, Work TM (1992) An outbreak of domoic acid poisoning attributed to the pennate diatom *Pseudonitzchia australis*. *J Phycol* 28(4):439–442.
11. Scholin CA, et al. (2000) Mortality of sea lions along the central California coast linked to a toxic diatom bloom. *Nature* 403(6765):80–84.
12. Rue E, Bruland K (2001) Domoic acid binds iron and copper: A possible role for the toxin produced by the marine diatom *Pseudo-nitzschia*. *Mar Chem* 76(1-2):127–134.
13. Bargu S, Lefebvre K, Silver MW (2006) Effect of dissolved domoic acid on the grazing rate of krill *Euphausia pacifica*. *Mar Ecol Prog Ser* 312:169–175.
14. Shaw BA, Andersen RJ, Harrison PJ (1997) Feeding deterrent and toxicity effects of apo-fucoxanthinoids and phycotoxins on a marine copepod (*Tigriopus californicus*). *Mar Biol* 128(2):273–280.
15. Bouillon R-C, Knierim TL, Kieber RJ, Skrabal SA, Wright JL (2006) Photodegradation of the algal toxin domoic acid in natural water matrices. *Limnol Oceanogr* 51(1):321–330.
16. Fisher JM, Reese JG, Pellechia PJ, Moeller PL, Ferry JL (2006) Role of Fe(III), phosphate, dissolved organic matter, and nitrate during the photodegradation of domoic acid in the marine environment. *Environ Sci Technol* 40(7):2200–2205.
17. Charlson RJ, Lovelock JE, Andreae MO, Warren SG (1987) Oceanic phytoplankton, atmospheric sulphur, cloud albedo and climate. *Nature* 326(6114):655–661.
18. Andreae MO, Raemdonck H (1983) Dimethyl sulfide in the surface ocean and the marine atmosphere: A global view. *Science* 221(4612):744–747.
19. Vallina SM, Simó R (2007) Strong relationship between DMS and the solar radiation dose over the global surface ocean. *Science* 315(5811):506–508.
20. Kieber DJ, Jiao J, Kiene RP, Bates TS (1996) Impact of dimethylsulfide photochemistry on methyl sulfur cycling in the equatorial Pacific Ocean. *J Geophys Res* 101(C2):3715–3722.
21. Bouillon R-C, Miller WL (2005) Photodegradation of dimethyl sulfide (DMS) in natural waters: Laboratory assessment of the nitrate-photolysis-induced DMS oxidation. *Environ Sci Technol* 39(24):9471–9477.
22. Bouillon R-C, Miller WL (2004) Determination of apparent quantum yield spectra of DMS photodegradation in an in situ iron-induced Northeast Pacific Ocean bloom. *Geophys Res Lett* 31(6), 10.1029/2004GL019536.
23. Brugger A, Slezak D, Obernosterer I, Herndl GJ (1998) Photolysis of dimethylsulfide in the northern Adriatic Sea: Dependence on substrate concentration, irradiance and DOC concentration. *Mar Chem* 59(3-4):321–331.
24. Toole DA, et al. (2004) High dimethylsulfide photolysis rates in nitrate-rich Antarctic waters. *Geophys Res Lett* 31(11):L11307.
25. Hasegawa K, Neta P (1978) Rate constants and mechanisms of reaction of Cl_2^- radicals. *J Phys Chem* 82(8):854–857.
26. Hiller KO, Asmus KD (1981) Oxidation of methionine by X_2^- in aqueous solution and characterization of some three-electron bonded intermediates. A pulse radiolysis study. *Int J Radiat Biol Relat Stud Phys Chem Med* 40(6):583–595.
27. Cory RM, Cotner JB, McNeill K (2009) Quantifying interactions between singlet oxygen and aquatic fulvic acids. *Environ Sci Technol* 43(3):718–723.
28. Halladja S, Ter Halle A, Aguer J-P, Boulkamh A, Richard C (2007) Inhibition of humic substances mediated photooxygenation of furfuryl alcohol by 2,4,6-trimethylphenol. Evidence for reactivity of the phenol with humic triplet excited states. *Environ Sci Technol* 41(17):6066–6073.
29. Zepp RG, Schlotzhauer PF, Sink RM (1985) Photosensitized transformations involving electronic energy transfer in natural waters: Role of humic substances. *Environ Sci Technol* 19(1):74–81.
30. Parker KM, Pignatello JJ, Mitch WA (2013) Influence of ionic strength on triplet-state natural organic matter loss by energy transfer and electron transfer pathways. *Environ Sci Technol* 47(19):10987–10994.
31. McGimpsey WG, Scaiano JC (1988) Photochemistry of α-chloro- and α-bromoacetophenone. Determination of extinction coefficients for halogen–benzene complexes. *Can J Chem* 66(6):1474–1478.
32. Bouillon R-C, Kieber RJ, Skrabal SA, Wright JL (2008) Photochemistry and identification of photodegradation products of the marine toxin domoic acid. *Mar Chem* 110(1-2): 18–27.
33. Grebel JE, Pignatello JJ, Mitch WA (2010) Effect of halide ions and carbonates on organic contaminant degradation by hydroxyl radical-based advanced oxidation processes in saline waters. *Environ Sci Technol* 44(17):6822–6828.
34. Treinin A, Loeff I, Hurley JK, Linschitz H (1983) Charge-transfer interactions of excited molecules with inorganic anions: The role of spin-orbit coupling in controlling net electron transfer. *Chem Phys Lett* 95(4-5):333–338.
35. Canonica S, Hellrung B, Wirz J (2000) Oxidation of phenols by triplet aromatic ketones in aqueous solution. *J Phys Chem A* 104(6):1226–1232.
36. Grebel JE, Pignatello JJ, Song W, Cooper WJ, Mitch WA (2009) Impact of halides on the photobleaching of dissolved organic matter. *Mar Chem* 115(1-2):134–144.
37. Méndez-Díaz JD, et al. (2014) Sunlight-driven photochemical halogenation of dissolved organic matter in seawater: A natural abiotic source of organobromine and organoiodine. *Environ Sci Technol* 48(13):7418–7427.
38. Leri AC, et al. (2015) A marine sink for chlorine in natural organic matter. *Nat Geosci* 8(8):620–624.
39. Keene WC, et al. (1998) Aerosol pH in the marine boundary layer: *A review and model evaluation*. *J Aerosol Sci* 29(3):339–356.
40. Finlayson-Pitts BJ (2003) The tropospheric chemistry of sea salt: A molecular-level view of the chemistry of NaCl and NaBr. *Chem Rev* 103(12):4801–4822.
41. Donati A (2002) Spectroscopic and kinetic investigations of halogen containing radicals in the tropospheric aqueous phase. PhD Thesis (Univ Leipzig, Leipzig, Germany).
42. Sander R, et al. (2003) Inorganic bromine in the marine boundary layer: A critical review. *Atmos Chem Phys* 3(5):1301–1336.
43. Holmes CD, et al. (2010) Global atmospheric model for mercury including oxidation by bromine atoms. *Atmos Chem Phys* 10(24):12037–12057.
44. Leifer A (1988) *The Kinetics of Environmental Aquatic Photochemistry: Theory and Practice* (American Chemical Society, Washington, DC).
45. Spinks JWT, Woods RJ (1990) *An Introduction to Radiation Chemistry* (Wiley-Interscience, New York), 3rd Ed.
46. Grebel JE, Pignatello JJ, Mitch WA (2011) Sorbic acid as a quantitative probe for the formation, scavenging and steady-state concentrations of the triplet-excited state of organic compounds. *Water Res* 45(19):6535–6544.
47. Takemoto T, Daigo K (1960) [On the constituents of *Chondria armata* and their pharmacological effect]. *Arch Pharm* 293(65):627–633. German.
48. Ianni JC (2012) *Kintecus, Windows Version 4.55* Available at www.kintecus.com. Accessed July 7, 2014.
49. Yang Y, Pignatello JJ, Ma J, Mitch WA (2014) Comparison of halide impacts on the efficiency of contaminant degradation by sulfate and hydroxyl radical-based advanced oxidation processes (AOPs). *Environ Sci Technol* 48(4):2344–2351.